in the range 10^8–10^9 M^{-1} s^{-1}. Rate constants for the reactions with olefins showed large variations with 1,1-dicyclopropyl- and 1,1-diphenylethylene being ca. 2 and 3 orders of magnitude, respectively, more reactive than oct-1-ene.

Acknowledgment. We thank Dr. C. Chatgilialoglu for helpful discussions and NATO for a research grant that made this possible and Dr. J. C. Scaiano for the use of the flash photolysis equipment.

Registry No. *t*-BuS, 16812-19-4; $Ph_2C{=}CH_2$, 530-48-3; $(c\text{-}C_3H_5)_2C{=}CH_2$, 822-93-5; Et_3B, 97-94-9; *s*-Bu_3B, 1113-78-6; $(MeO)_3P$, 121-45-9; $(EtO)_3P$, 122-52-1; Bu_3P, 998-40-3; oct-1-ene, 111-66-0.

Kinetically Stable Complexes of Alkali Cations with Rigidified Calix[4]arenes: Synthesis, X-ray Structures, and Complexation of Calixcrowns and Calixspherands

Pieter J. Dijkstra,[†] Jos A. J. Brunink,[†] Kjell-Erik Bugge,[†] David N. Reinhoudt,*[,†] Sybolt Harkema,[‡] Rocco Ungaro,[§] Franco Ugozzoli,[§] and Eleonora Ghidini[§]

Contribution from the Laboratories of Organic Chemistry and Chemical Physics, University of Twente, 7500 AE Enschede, The Netherlands, and Institute of Organic Chemistry, University of Parma, 43100 Parma, Italy. *Received February 13, 1989*

Abstract: Selective 1,3-dialkylation of the phenolic groups of *p-tert*-butylcalix[4]arene (**3**) with methyl or benzyl tosylate yields **7a** (75%) and **8** (95%), respectively. Subsequent bridging of the two remaining phenolic groups in **7a** or **8**, by reaction with polyethylene glycol ditosylates, gives *p-tert*-butylcalix[4]arene crown ethers (**4b**, **4c**, and **4e**). Reaction of **7a** with 3,3″-bis(bromomethyl)-2,2′,2″-trimethoxy-5,5′,5″-trimethyl-1,1′:3′,1″-terphenyl (**10**) in the presence of NaH or KH produces the corresponding NaBr and KBr complexes of the calixspherand **6**. Decomplexation of the **6**·NaBr and **6**·KBr complexes in H_2O/CH_3OH (4:1) requires long reaction times and high temperatures, indicating a high *kinetic* stability. The X-ray structure of **6**·NaPic confirmed the flattened partial cone conformation of the calixarene moiety in this complex. The free energies of complexation ($\Delta G°$) of the calixcrown ether alkali picrate (MPic) complexes vary from −6 to −12 kcal·mol^{-1} ($CDCl_3$). The calixspherand **6** forms kinetically "stable" complexes with Na^+ ($k_d^{298} = 6.0 \times 10^{-9}$ s^{-1}), K^+ ($k_d^{298} = 1.0 \times 10^{-8}$ s^{-1}), and Rb^+ ($k_d^{298} = 6.9 \times 10^{-5}$ s^{-1}). The rates of complexation vary between 1.3×10^4 and 2.5×10^5 M^{-1}·s^{-1}. The calculated free energies of complexation of **6** with MPic salts in $CDCl_3$ at 298 K are −16.8 (**6**·Na^+), −18.1 (**6**·K^+), and −13.0 (**6**·Rb^+) kcal·mol^{-1}, respectively. The high thermodynamic and kinetic stabilities of these complexes are explained in terms of a high degree of preorganization of the calixspherand and the highly hydrophobic collar around the molecular cavity. This prevents solvent molecules to assist in the decomplexation process.

The thermodynamic and kinetic stabilities of the alkali cation complexes of macrocyclic polyethers incorporating meta-coupled anisyl (or anisyl and cyclic urea) units have been studied in detail by Cram et al.[1] Increased substitution of ethyleneoxy moieties in crown ethers by meta-coupled anisyl units enhances the thermodynamic stability of the corresponding alkali cation complexes. The result of the work of Cram and co-workers on the effect of anisyl oxygen atoms as ligating sites can be summarized in the following statement about preorganization: "the more highly hosts and guests are organized for binding and for low solvation prior to their complexation, the more stable will be their complexes".[1] The spherands (e.g., **1** (Chart I)) are the ultimate demonstration of the preorganization principle, and spherand **1** is the best host for the small alkali cations Li^+ and Na^+. Spherand **1** rejects the larger alkali cations K^+, Rb^+, and Cs^+.

The preorganization principle not only affects the *thermodynamic* stability but also has a pronounced effect on the *kinetic* stability of the alkali complexes of the spherands. The anisyl groups in the spherands provide the preorganized ligating donor sites, and they shield the cavity from solvent molecules. As a result, the rates of complexation by the spherands are decreased and the rates of decomplexation are even more decreased, when compared with flexible crown ethers. Slow decomplexation on the human time scale of alkali cation complexes is limited to the anisyl spherands like **1**, but these spherands only complex Li^+ and Na^+ ions.

Chart I[a]

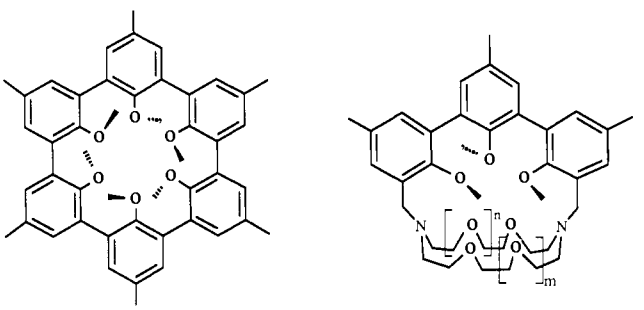

1

2
a, m=n=2
b, m=2, n=1
c, m=n=1

[a] The bars at the phenyl rings and at the oxygen atoms indicate methyl groups.

Our interest in macrocyclic host molecules with preorganized cavities is related to the possible application of radioactive Rb^+ isotopes in organ imaging. Therefore, we have focused our work on the synthesis of spherand-type host molecules that have a larger

[†] Laboratory of Organic Chemistry, University of Twente.
[‡] Laboratory of Chemical Physics, University of Twente.
[§] Institute of Organic Chemistry, University of Parma.

(1) (a) Cram, D. J.; Kaneda, T.; Helgeson, R. C.; Brown, S. B.; Knobler, C. B.; Maverick, E.; Trueblood, K. N. *J. Am. Chem. Soc.* **1985**, *107*, 3645–3657. (b) Cram, D. J.; Lein, G. M. *J. Am. Chem. Soc.* **1985**, *107*, 3657–3668.

0002-7863/89/1511-7567$01.50/0

Table I. Selected Chemical Shifts (δ) of Cryptahemispherand **2a** Complexes of Sodium, Potassium, and Rubidium Chlorides in $CDCl_3$ (25 °C)

	2a·NaCl	**2a**·KCl	**2a**·RbCl
$ArCH_3$ (inner)	2.42	2.45	2.45
$ArCH_3$ (outer)	2.34	2.37	2.37
$ArOCH_3$ (inner)	2.84	2.82	2.77
$ArOCH_3$ (outer)	3.36	3.36	3.36

cavity and resemble the spherands in their kinetic stability. Previously we have reported variations in the structures of hemispherands, composed of a rigid terphenyl or 2,6-diarylpyridine moiety and a flexible polyether chain.[2-5] Although these compounds form thermodynamically relatively stable complexes with Rb^+, even on the ^1H NMR time scale, the rate of decomplexation is fast.

Results and Discussion[6]

CPK molecular models of *bicyclic* host compounds incorporating the *m*-teranisyl moiety revealed the possibility to construct rigid macrocycles with cavities with varying diameters. A CPK molecular model of the *m*-teranisyl-bridged diaza-18-crown-6, recently referred to as a cryptahemispherand, indicated complementarity with the larger alkali cations K^+, Rb^+, and Cs^+. With smaller diazacrown ethers, such cryptahemispherands give rise to smaller cavities complementary with Li^+, Na^+, and probably K^+ cations. At the time we had decided to synthesize the cryptahemispherand **2a** and to study the thermodynamic and kinetic stabilities of the corresponding complexes of the macrocycle, we learned that cryptahemispherands **2a–c** had already been synthesized by Cram and co-workers.[7] They had determined the association constants of the complexes of these cryptahemispherands in chloroform saturated with water. The K_a values of the **2a** and **2c** complexes with Rb^+ are 7.72×10^{14} (for **2a**) and 5.67×10^9 $L \cdot mol^{-1}$ (for **2c**).

Although the kinetic stability (rates of decomplexation) of the alkali complexes of the cryptahemispherands was not reported by Cram et al., these macrocycles should be kinetically stable, at least in *apolar* solvents like chloroform, even when the rates of complexation are diffusion controlled ($k_c \approx 10^8$–10^9 $M^{-1} \cdot s^{-1}$). The cryptahemispherand **2a**, having a cavity complementary with the larger alkali cations (K^+, Rb^+, and Cs^+), was synthesized according to the procedure described by Cram and co-workers.[7] Because the cryptahemispherands are not very stable, the correspondingly more stable borane complexes were prepared and stored. The free ligand **2a** was prepared from the borane complex and subsequently complexed with RbCl to give **2a**·RbCl.

In order to determine the kinetic stability of this complex, a homogeneous solution of **2a**·RbCl (0.001 M), NaCl (0.150 M), and KCl (0.030 M) in 100 mL of water at pH 7.4 (Ringers solution) was stirred at room temperature. The exchange of Rb^+ for Na^+ and K^+ was monitored by ^1H NMR according to the following procedure. Samples (10 mL) of the solution were run over a SEP-PACK column to separate the complexes from the free salts by washing with water. The cryptahemispherand complexes that remained on the column were eluted with methanol, and the methanol was evaporated. A ^1H NMR spectrum of a $CDCl_3$ solution of the cryptahemispherand complexes (Table I) gave the ratio of K^+ and Rb^+ from the OCH_3 signals at δ 2.82 and 2.77, respectively. We found that Rb^+ is exchanged for Na^+ and K^+. The ^1H NMR spectra ($CDCl_3$) recorded after 10 min showed two signals for the outer $ArCH_3$ groups and two signals for the inner $ArCH_3$ groups, both in a 1:1 ratio. Obviously, a rapid exchange to the Na^+ complex takes place because of the large excess of Na^+ present. This was confirmed by the three signals of the inner OCH_3 protons of the *m*-teranisyl moiety, indicating that the **2a**·NaCl, **2a**·KCl, and **2a**·RbCl complexes are present. The ^1H NMR spectra recorded of samples after longer periods of equilibrium showed an increase of the **2a**·KCl complex relative to the Rb^+ complex as well as the Na^+ complex. After 2 h, an equilibrium was established with almost exclusively the K^+ complex present (K^+/Na^+ and $K^+/Rb^+ \geq 30{:}1$).

Obviously, the rate of decomplexation of the cryptahemispherand–RbCl complex in water resembles the rate of decomplexation of K^+–cryptand complexes[8] and is much higher than the expected rate in chloroform that we had calculated from the association constant (vide supra). There are at least two reasons that might explain this high rate of exchange with K^+ or Na^+ ions in aqueous solution. Firstly, the ion exchange may take place via a bimolecular process instead of a simple dissociation of the **2a**·Rb^+ complex as the rate-determining step. Previously we have shown that bimolecular exchange processes contribute substantially to the overall exchange of cations in complexes of crown ethers and *tert*-butylammonium salts.[9] Secondly, Cox et al.[8] showed that the rate of decomplexation of the alkali cation complexes of cryptands depends strongly on the solvent. This is due to the solvation of the ligating sites and the complexed cation, and the rates of decomplexation increase with increasing solvent donicity. In the spherands, this solvation is strongly inhibited by the aromatic rings and the six alternating methoxy groups of the anisole moieties, but this is not the case in the cryptahemispherands that have a much more accessible molecular cavity.

Irrespective of which of these two factors contributes most, only complexes of ligands with a sterically less accessible cavity will exhibit a higher kinetic stability. Therefore, the further objective of our work was to design and synthesize ligands with a rigid molecular cavity that is both sufficiently large for Rb^+ and sufficiently shielded from the solvent by a hydrophobic collar of hydrocarbon moieties.

Calixcrowns and Calixspherands

Design. CPK molecular models show that the molecular framework of the calix[4]arene (**3**) becomes more rigid when the phenolic oxygen atoms are alkylated. Therefore, we decided to use the 1,3-dialkylated calix[4]arene moiety as a bridge to construct bicyclic macrocycles that are comparable with the cryptahemispherands. The 1,3-dialkoxy-*p*-*tert*-butylcalix[4]arene moiety shields the cavity from solvent molecules by the aryl, methylene, and alkyl groups present. CPK molecular models of the 1,3-dimethoxy-*p*-*tert*-butylcalix[4]arene-crown-5 (**4b**), which combines a 16- with a 22-membered ring, indicate that the aryl units are conformationally mobile. Inversion of one or two units renders interconversion of the cone, the partial cone, and the 1,3-alternate conformations possible. This conformational freedom will be reduced in the 1,3-bis(benzyloxy)-*p*-*tert*-butylcalix[4]arene-crown-5 (**4c**). Bridging of the calix[4]arenes with a 2,6-dianisylpyridine or a *m*-teranisyl moiety leads to almost completely fixed molecules (**5** and **6**, respectively). The molecular framework of these compounds also provides a cavity lined by aryl, methylene,

(2) Dijkstra, P. J.; den Hertog, H. J., Jr.; van Steen, B. J.; Zijlstra, S.; Skowronska-Ptasinska, M.; Reinhoudt, D. N.; van Eerden, J.; Harkema, S. *J. Org. Chem.* **1987**, *52*, 2433–2442.

(3) Dijkstra, P. J.; Skowronska-Ptasinska, M.; Reinhoudt, D. N.; den Hertog, H. J., Jr.; van Eerden, J.; Harkema, S.; de Zeeuw, D. *J. Org. Chem.* **1987**, *52*, 4913–4921.

(4) Dijkstra, P. J.; den Hertog, H. J., Jr.; van Eerden, J.; Harkema, S.; Reinhoudt, D. N. *J. Org. Chem.* **1988**, *53*, 374–376.

(5) Dijkstra, P. J.; van Steen, B. J.; Hams, B. H. M.; den Hertog, H. J., Jr.; Reinhoudt, D. N. *Tetrahedron Lett.* **1986**, *27*, 3183–3186.

(6) Some preliminary results of this work have been published: Reinhoudt, D. N.; Dijkstra, P. J.; in 't Veld, P. J. A.; Bugge, K. -E.; Harkema, S.; Ungaro, R.; Ghidini, E. *J. Am. Chem. Soc.* **1987**, *109*, 4761–4762.

(7) (a) Cram, D. J.; Ho, S. P.; Knobler, C. B.; Maverick, E.; Trueblood, K. N. *J. Am. Chem. Soc.* **1986**, *108*, 2989–2998. (b) Cram, D. J.; Ho, S. P. *J. Am. Chem. Soc.* **1986**, *108*, 2998–3005. We thank Professor D. J. Cram for detailed information about the synthesis of cryptahemispherands prior to publication.

(8) Cox, B. G.; Garcia-Rosas, J.; Schneider, H. *J. Am. Chem. Soc.* **1981**, *103*, 1054–1059, 1384–1389. Cox et al. showed that the rate of decomplexation of the alkali cation complexes of the cryptands depends strongly on the solvent. This is due to the solvation of the ligating sites and the complexed cation, and rates of decomplexation increase with increasing solvent polarity. CPK models of **2a** reveal that this solvation is *partly* inhibited by the *m*-teranisyl moiety, of which the aromatic rings and the outwardly pointing methoxy methyl groups shield the cavity.

(9) Reinhoudt, D. N.; de Jong, F. *Progress in Macrocyclic Chemistry*; Izatt, R. M., Christensen, J. J., Eds.; Wiley: New York, 1979; Vol. I, p 157–217.

and methyl groups. Consequently, the oxygen-ligating sites are largely shielded from solvent molecules. Therefore, these compounds will be different from the cryptahemispherands in terms of desolvation and reorganization of the host upon complexation.

Synthesis. The base-catalyzed condensation of *p-tert*-butylphenol and formaldehyde to give *p-tert*-butylcalix[4]arene (**3**) has recently been studied by Gutsche and co-workers[10] to establish a general laboratory procedure. Using this procedure, we obtained reproducible yields of 40–44%. The phenolic OH groups of **3** can be readily converted in the corresponding alkyl ethers by reaction with alkyl halides and base, but *selective* alkylation has only been reported in a few cases.[11] We found that the reaction of **3** with diazomethane gives a mixture of mono-, di-, tri-, and tetramethoxy-*p-tert*-butylcalix[4]arenes. Gutsche and co-workers have described that *p*-allylcalix[4]arene with benzyl tosylate gives the 1,3-benzylated product. We found that reaction of **3** with methyl tosylate in THF and sodium hydride as a base afforded a mixture of the monomethyl ether (20%), and 1,3-dimethyl ether (**7a**, 32%) together with unreacted **3**. The yield of **7a** could be increased to 75% when the reaction of **3** with methyl tosylate was performed in acetone with K_2CO_3 as a base. We also obtained 1,3-bis(benzyloxy)-*p-tert*-butylcalix[4]arene (**8**) in 95% yield by reaction of **3** with benzyl tosylate in acetone and with sodium hydride as a base. In the ^1H NMR spectrum of **8**, the presence of an AB system for the benzylic protons ($ArCH_2Ar$) and two singlets for the *tert*-butyl hydrogen atoms at δ 1.29 and 0.94, respectively, showed that **8** is present in a cone conformation.

Previously we[12] reported the synthesis of *p-tert*-butylcalix[4]arene-crown-5 (**4a**) and -crown-6 (**4d**) by reacting **3** with the appropriate polyethylene glycol ditosylate and a base (Chart II). When bicyclic crown ethers **4a** and **4d** were methylated with dimethyl sulfate in THF, **4b** and **4e** were obtained in yields of 60% and 75%, respectively. When **7a** was reacted with tetraethylene glycol ditosylate in THF in the presence of sodium hydride, the calixcrown ether **4b** was formed in 30% yield. The calixcrown-6 (**4e**) was synthesized by reaction of **7a** and pentaethylene glycol ditosylate in 50% yield. The products obtained via the two different routes showed identical ^1H NMR spectra, indicating that the conformations are the same. The 1,3-bis(benzyloxy)-*p-tert*-butylcalix[4]arene-crown-5 (**4c**) was prepared from **8** in 25% yield in the same way as described for **4b**. The ^1H NMR spectra ($CDCl_3$) of **4b**, **4c**, and **4e** showed an AB system for the benzylic protons, and two distinct singlets for the *tert*-butyl protons (1:1 ratio). This revealed that the calix[4]arene crown ethers are present in a cone conformation.

Previously we[2] described the synthesis of a pyridohemispherand with a modified inner sphere from the building block **9**. The macrocyclization reaction of **9** and **7a** in THF and sodium hydride as a base afforded the novel host **5** in 20% yield. In the ^1H NMR spectrum ($CDCl_3$), the *tert*-butyl protons are present at δ 1.48 and 0.82 in a 1:1 ratio corresponding to a cone conformation of the *p-tert*-butylcalix[4]arene moiety. The absorptions of the methoxy groups in the 2,6-dianisylpyridine and the *p-tert*-butylcalix[4]arene moieties coincide at δ 3.27. The benzylic protons ($ArCH_2O$) appear as an AB system (J = 8.6 Hz) at δ 5.44 and 4.20, indicating that the inversion of the 2,6-dianisylpyridine moiety is slow on the ^1H NMR time scale. Obviously, in **5** the rotation of anisyl units through the cavity which has been observed in the pyridine hemispherand is now restricted.

Reaction of 3,3″-bis(bromomethyl)-2,2′,2″-trimethoxy-5,5′,5″-trimethyl-1,1′:3′,1″-terphenyl (**10**),[13] which preserves an alternating arrangement of the methoxy groups during synthesis, with **7a** and sodium hydride in THF afforded **6**·NaBr in 23% yield. We could not simply remove the complexed NaBr from this

Chart II

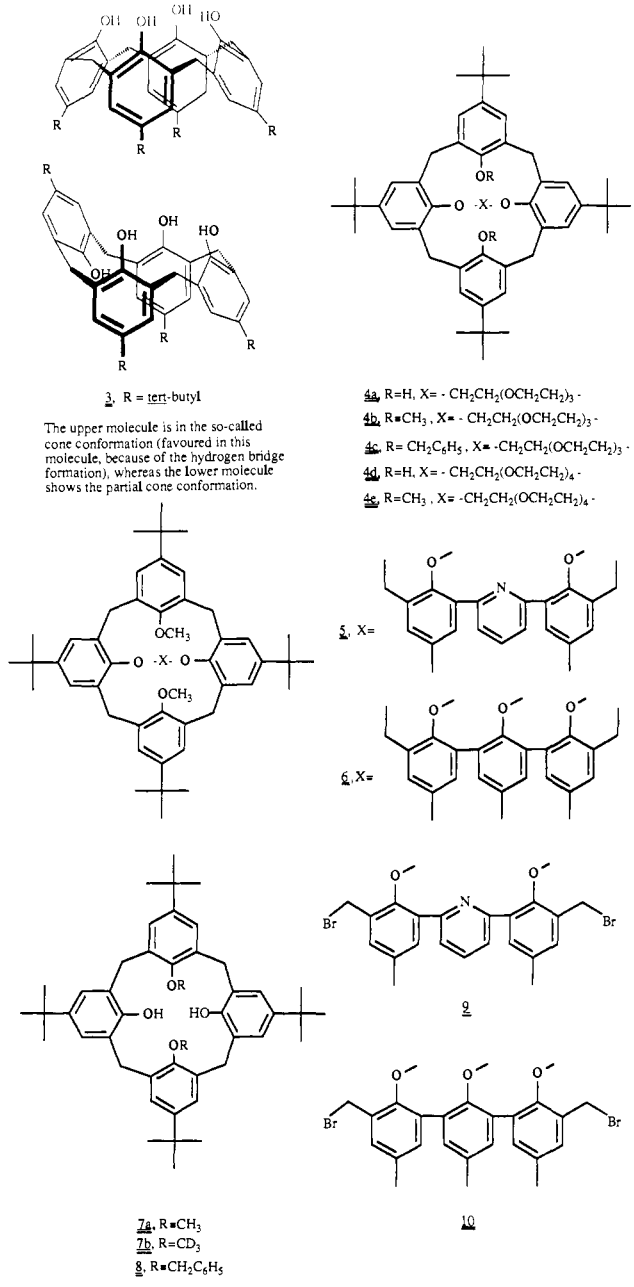

complex by heating a mixture of **6**·NaBr in methanol/water (1:4), and this behaviour strongly resembles that of the spherand **1**·LiCl and **1**·NaCl complexes. The spherand **1**·LiCl complex could only be decomplexed by Cram et al. in a 1:4 methanol/water mixture in a sealed ampule at 120 °C. The driving force of the decomplexation is the insolubility of **1** in this solvent mixture. This methodology, which shifts the equilibrium to the uncomplexed molecule **1**, was also applied to **6**·NaBr. As expected, the hydrophobicity of the *p-tert*-butylcalix[4]arene bridged with the *m*-teranisyl unit renders the molecule insoluble in water and methanol contrary to the **6**·NaBr complex, which is soluble in methanol. After approximately 3 days of heating of a suspension of **6**·NaBr in methanol water (1:4) in a sealed ampule at 120 °C, decomplexation to the free ligand **6** was complete.

In order to investigate a possible template effect in the reaction of **10** and **7a**, the reaction was performed under the same conditions as described for the synthesis of **6**·NaBr, substituting the base either for LiH or KH. The reaction with LiH did not give **6**·LiBr or **6**, but the reaction with KH afforded the potassium bromide complex **6**·KBr in 5–9% yield. Decomplexation of the potassium bromide complex **6**·KBr to the free ligand **6** appeared to be more easy than that of **6**·NaBr. When a suspension of **6**·KBr

(10) Gutsche, C. D.; Iqbal, M.; Stewart, D. *J. Org. Chem.* **1986**, *51*, 742–745.
(11) Gutsche, C. D.; Dhawan, B.; Levine, J. A.; No, K. H.; Bauer, L. J. *Tetrahedron* **1983**, *39*, 409–426.
(12) (a) Alfieri, G.; Dradi, E.; Pochini, A.; Ungaro, R.; Andreetti, G. D. *J. Chem. Soc., Chem. Commun.* **1983**, 1075–1077. (b) Ungaro, R.; Pochini, A.; Andreetti, G. D. *J. Inclusion Phenom.* **1984**, *2*, 199–206.
(13) Lein, G. M.; Cram, D. J. *J. Am. Chem. Soc.* **1985**, *107*, 448–455.

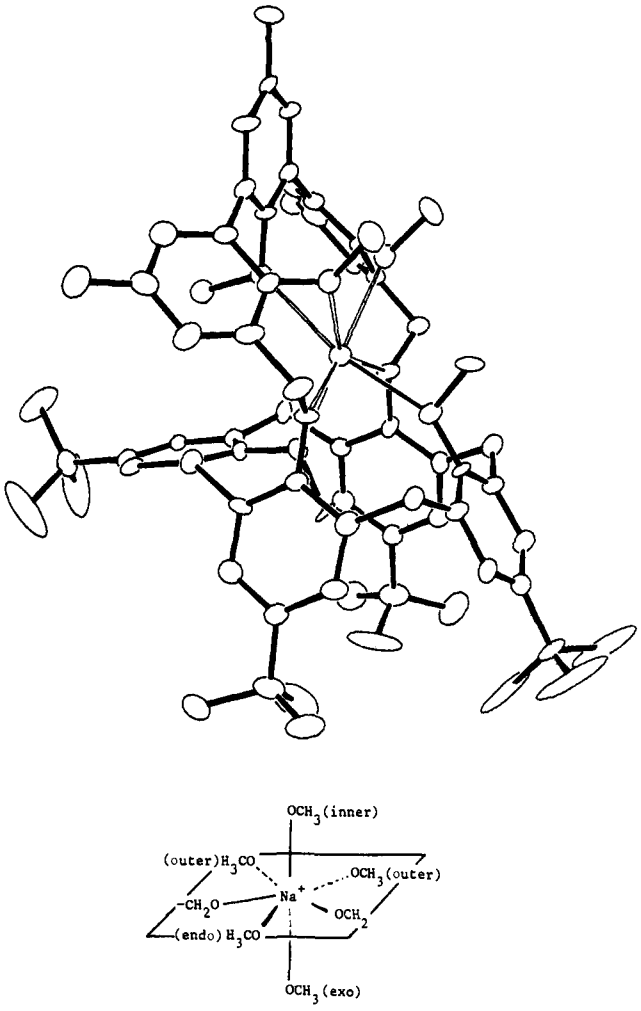

Figure 1. Crystal structure of **6**·Na^+. The molecule has a minor plane as a crystallographic symmetry element.

was refluxed for 3 days in a 1:4 methanol/water mixture, the free ligand **6** was isolated quantitatively.

Crystal Structure of 6·NaPic. Because **6**·NaBr was difficult to crystallize, we exchanged the bromine anion in **6**·NaBr for the picrate anion. Crystallization of **6**·NaPic from a mixture of chloroform and methanol by slow evaporation afforded crystals suitable for X-ray analysis. The structure of the sodium picrate complex of **6** was determined by X-ray crystallography. An ORTEP[14] view of the structure is given in Figure 1. The asymmetric unit contains half a molecule, the other half being generated by a mirror plane. The picrate ion, which is not bonded to the Na^+ ion, is disordered. The complete data of the crystallographic studies have been deposited.[6] The structure shows that the Na^+ ion is encapsulated in a cavity formed by the alternating arrangement of the three methoxy oxygen atoms of the *m*-teranisyl moiety and the four oxygen atoms of the 1,3-dimethoxy-*p*-*tert*-butylcalix[4]arene moiety, which has a flattened partial cone conformation. As a result, the arrangement of donor atoms around the Na^+ ion is an approximate pentagonal bipyramid. The Na^+–O and the O–O distances in the molecule are given in Table II. The aryl–aryl dihedral angle of the *m*-teranisyl moiety is 54.7°, close to the value found in the spherand **1**·NaCl complex (56°).[1] The Na^+···O distances vary from 2.4 to 2.6 Å, giving a cavity of ~2.2 Å, in between the ionic diameters of Na^+ (1.96 Å) and K^+ (2.66 Å).

(14) Johnson, C. K. ORTEP. Report ORNL-3794, 1965; Oak Ridge National Laboratory, Oak Ridge, TN.
(15) Noyes, R. M. *J. Am. Chem. Soc.* **1962**, *84*, 513–522.

Table II. Calixspherand Dimensions in the Crystal Structure of the NaPic Complex of Ligand **6**

	6·NaPic
Na^+···O Distances, Å	
calix[4]arene	
Na^+···OCH_2	2.60
Na^+···OCH_3 (exo)	2.43
Na^+···OCH_3 (endo)	2.38
m-teranisyl	
Na^+···OCH_3 (outer)	2.58
Na^+···OCH_3 (inner)	2.51
Distances between O atoms, Å	
calix[4]arene	
OCH_2···OCH_2	4.92
OCH_2···OCH_3 (exo)	3.07
OCH_2···OCH_3 (endo)	3.12
OCH_3 (exo)···OCH_3 (endo)	3.30
m-teranisyl	
OCH_3 (outer-outer)	3.30
OCH_3 (outer-inner)	2.82
inner OCH_3–endo OCH_3	4.86

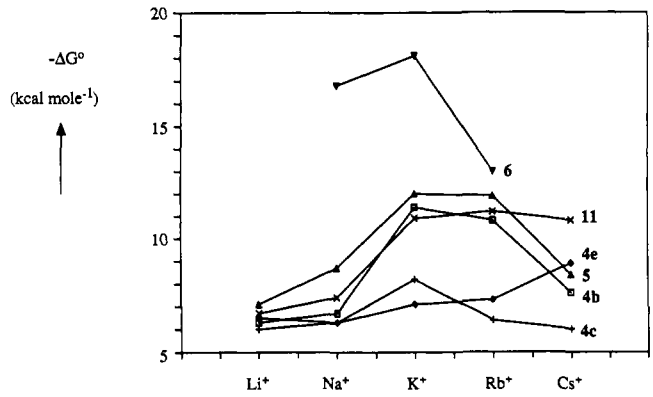

Figure 2. Gibbs free energy ($-\Delta G°$) of alkali cation complexation.

A CPK molecular model of the spherand **6** shows that the cavity is the most complementary to K^+, and the flattened partial cone conformation of the *p*-*tert*-butylcalix[4]arene moiety the most favorable. Whereas the three methoxy groups that are on the same face of the molecule do not show that steric constraints are present, the central methoxy group of the *m*-teranisyl moiety in **6** serves as a steric barrier for the inverted anisyl group of the *p*-*tert*-butylcalix[4]arene moiety. The steric barrier resulting from this central methoxy is absent in hosts **4b**, **4e**, and **5**. Rotations to convert a cone into a partial cone conformation are possible in **4b** and **5**, taking into account the overestimation in these CPK molecular models of the steric barriers in conformational changes.

Complexation Studies

Thermodynamic Stabilities of the Complexes. The association constants (K_a) and binding free energies ($\Delta G°$) of the 1,3-dialkoxy-*p*-*tert*-butylcalix[4]arene crown ethers **4b**, **4c**, and **4e** and the 2,6-dianisylpyridine–*p*-*tert*-butylcalix[4]arene (**5**) were determined by the two-phase (water, chloroform) picrate extraction method.[1] The K_a (M^{-1}) and $-\Delta G°$ (kcal·mol^{-1}) values obtained are presented in Table III. The macrobicyclic crown **4b** shows peak selectivity for potassium and rubidium picrate with $\Delta G°$ values of −11.4 and −10.8 kcal·mol^{-1}, respectively (see Figure 2). The ^1H NMR spectra recorded of the organic phases after extraction reveal the conformational changes of the 1,3-dimethoxy-*p*-*tert*-butylcalix[4]arene-crown-5 (**4b**) upon complexation of potassium and rubidium picrate salts. The ^1H NMR spectrum of the free ligand shows that the *p*-*tert*-butylcalix[4]arene moiety is in the cone conformation (vide supra). However, upon complexation, the spectrum of the 1,3-dimethoxy-*p*-*tert*-butylcalix-

Table III. Association Constants (K_a) and Binding Free Energies ($-\Delta G°$) of Complexes of Hosts with Alkali Picrates in $CDCl_3$ Saturated with H_2O at 22 °C[a,b]

	K_a, M^{-1}					$-\Delta G°$, kcal·mol^{-1}				
compd	Li^+	Na^+	K^+	Rb^+	Cs^+	Li^+	Na^+	K^+	Rb^+	Cs^+
4b	3.8×10^4	1.1×10^5	3.0×10^8	1.1×10^8	4.7×10^5	6.3	6.7	11.4	10.8	7.6
4c	$<10^4$	4.3×10^4	1.2×10^6	5.9×10^4	$<10^4$	<6	6.3	8.2	6.4	<6
4e	5.5×10^4	4.2×10^4	1.5×10^5	2.1×10^5	3.2×10^6	6.5	6.3	7.1	7.3	8.9
5	2.1×10^5	3.1×10^6	8.2×10^8	6.2×10^8	1.8×10^6	7.1	8.7	12.0	11.9	8.4
11	8.5×10^4	2.8×10^5	9.3×10^7	1.6×10^8	8.5×10^7	6.7	7.4	10.9	11.2	10.8

[a] The association constants were determined as described by Cram et al.[1] [b] The association constants of **6** could not be determined by two-phase extraction because no equilibrium could be reached, except in the case of rubidium picrate; see Table V.

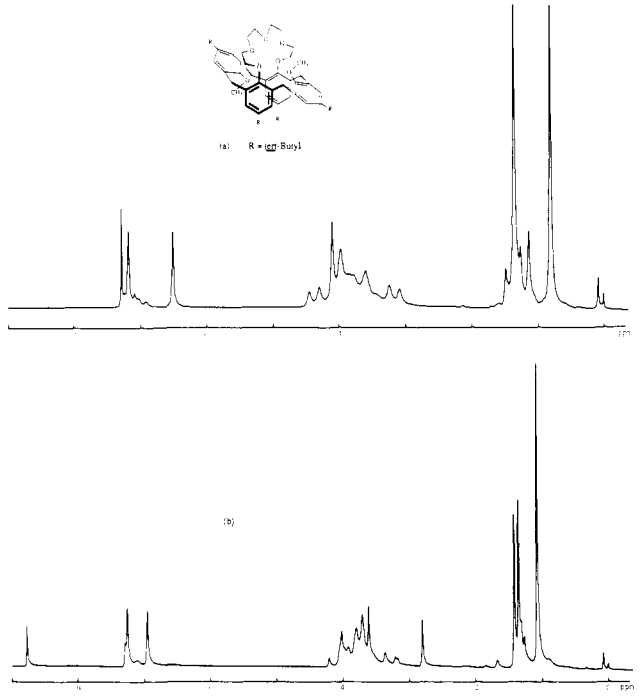

Figure 3. ^1H NMR spectra ($CDCl_3$) of **4b** (a) and **4b**·KPic (b).

[4]arene-crown-5-potassium picrate complex (≥90% complexation) revealed a flattened partial cone conformation, as indicated by the 1:1:2 ratio of the signals of the *tert*-butyl groups (Figure 3). The complex of **4b** with rubidium picrate (~85% complexation) also showed a flattened partial cone conformation of the calix[4]arene moiety as indicated by the 1:1:2 ratio of the signal of the *tert*-butyl groups.

The ^1H NMR spectra of the **4e**·MPic complexes are very similar. The interpretation of these ^1H NMR data was supported by the X-ray structure determination of the RbPic complex of **4e**. The structure given in Figure 4 clearly shows that the *p-tert*-butylcalix[4]arene moiety has a conformation in between a cone and a partial cone ("flattened partial cone"). Bond distances, bond angles, and selected torsion angles are presented in Table IV. Complete lists of the structural parameters have been deposited as supplementary material.

The analysis of the thermal parameters shows that the crown section C7*–C8* is disordered between two different positions with occupancy factors of 0.6 and 0.4, respectively. A difference with the **6**·NaPic complex is the participation of the picrate anion in the coordination of the Rb^+ cation which is further surrounded by four phenolic oxygens and four oxygens of the polyether chain. The strongest Rb–O (2.90 Å) interaction is with the picrate anion. Other Rb–O distances are larger, with the Rb–O12* distance being as long as 3.43 Å.

The conformation of the crown can be described by the torsion angles O–C–C–O, which are all close to 60° with the exception of the O6*–C7*–C8*–O9* moiety of the disordered part. The *p-tert*-butylcalix[4]arene structure is best described by the dihedral angles formed by the phenolic units and the weighted least-squares planes through the four methylene bridges as a reference plane R (A–R 2.3 (3)°, B–R 80.5 (3)°, C–R 52.5 (3)°, D–R 80.6 (3)°),

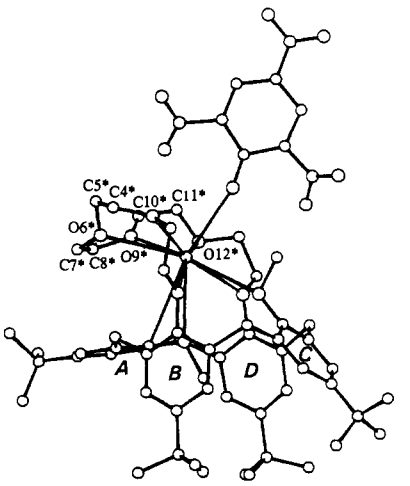

Figure 4. Crystal structure of **4e**·RbPic.

Table IV. Bond Distances (Å), Bond Angles (deg), and Selected Torsion Angles (deg) Involving the Rb Atom

	Bond Distances, Å		
Rb1–O1A	2.944 (8)	Rb1–O6*	3.11 (1)
Rb1–O1B	3.078 (9)	Rb1–O9*	2.96 (1)
Rb1–O1C	3.136 (8)	Rb1–O12*	3.43 (1)
Rb1–O1D	3.051 (8)	Rb1–O7G	2.90 (1)
Rb1–O3*	3.00 (1)		
	Bond Angles, deg		
O9*–Rb1–O7G	98.4 (3)	O1C–Rb1–O1D	64.4 (2)
O6*–Rb1–O7G	109.7 (4)	O1B–Rb1–O7G	114.4 (3)
O6*–Rb1–O9*	54.0 (4)	O1B–Rb1–O9*	133.6 (3)
O3*–Rb1–O7G	81.2 (3)	O1B–Rb1–O6*	83.4 (3)
O3*–Rb1–O9*	101.6 (3)	O1B–Rb1–O3*	55.6 (3)
O3*–Rb1–O6*	53.4 (3)	O1B–Rb1—O1D	117.5 (2)
O1D–Rb1–O7G	88.6 (3)	O1B–Rb1–O1C	61.7 (2)
O1D–Rb1–O9*	94.1 (3)	O1A–Rb1–O7G	147.4 (2)
O1D–Rb1–O6*	144.3 (4)	O1A–Rb1–O9*	103.5 (3)
O1D–Rb1–O3*	162.3 (3)	O1A–Rb1–O6*	102.7 (4)
O1C–Rb1–O7G	84.3 (3)	O1A–Rb1–O3*	116.9 (3)
O1C–Rb1–O9*	158.3 (3)	O1A–Rb1–O1D	66.1 (2)
O1C–Rb1–O6*	145.0 (3)	O1A–Rb1–O1C	66.6 (6)
O1C–Rb1–O3*	100.1 (2)	O1A–Rb1–O1B	65.2 (2)
	Selected Torsion Angles, deg		
O1B–C1*–C2*–O3*	59 (2)	C7*–C8*–O9*–C10*	−137 (5)
C1*–C2*–O3*–C4*	80 (2)	C8*–O9*–C10*–C11*	−178 (3)
C2*–O3*–C4*–C5*	−171 (2)	O9*–C10*–C11*–O12*	56 (2)
O3*–C4*–C5*–O6*	60 (2)	C10*–C11*–O12*–C13*	166 (2)
C4*–C5*–O6*–C7*	159 (2)	C11*–O12*–C13*–C14*	178 (1)
C5*–O6*–C7*–C8*	109 (4)	O12*–C13*–C14*–O1D	−68 (2)
O6*–C7*–C8*–O9*	−4 (7)		

and by the dihedral angles formed by each phenolic unit and the adjacent one (A–B 80.4 (4)°, B–C 84.0 (4)°, C–D 83.3 (4)°, D–A 80.8 (4)°).

Upon complexation of **4b** with potassium picrate in different ratios, the ^1H NMR spectra ($CDCl_3$) showed the free and complexed ligand present. Obviously the decomplexation rate becomes slow on the 80-MHz ^1H NMR time scale.

When the complexation of 1,3-dimethoxy-*p-tert*-butylcalix[4]arene-crown-5 (**4b**) with alkali picrates under two-phase partition ($CDCl_3/H_2O$) is compared with the 21-membered

Chart III

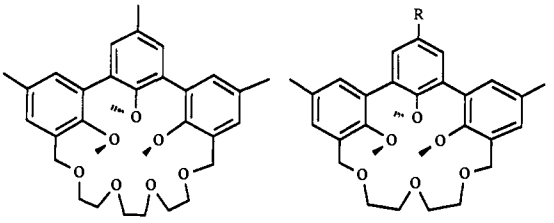

11 12a R = $C(O)CH_3$ 12b R = CH_3

hemispherand **11** (Chart III), we can see that both hosts are complementary with the K^+ and Rb^+ cations (Table III), with binding free energies of ~11.0 kcal·mol^{-1}. Previously we have shown that **11** is an equally good binder of potassium and rubidium picrate compared to the more rigid hemispherand with *four* meta-coupled anisyl units in a 21-membered ring.[2] The 1,3-dimethoxy-*p-tert*-butylcalix[4]arene-crown-5 (**4b**) seems to be flexible, but the selectivity toward alkali picrate complexation differs from **11**. Whereas **11** shows a K^+/Na^+ selectivity of 330, this value is increased in **4b** (2.8×10^3) by almost a factor 10. Host **4b** also shows a large decrease in binding free energies for the larger alkali cations ($\Delta\Delta G°$(rubidium/cesium picrate) = 3.2 kcal·mol^{-1}). The more pronounced peak selectivity of **4b** compared with **11** is attributed to the *macrobicyclic* effect, which also is found in the diazacryptands.

Surprisingly, the increased rigidity introduced by the benzyloxy groups in **4c** compared to the methoxy groups in **4b** *lowers* the binding free energies substantially for K^+ ($\Delta\Delta G°$ = 3.2 kcal·mol^{-1}) and for Rb^+ ($\Delta\Delta G°$ = 4.3 kcal·mol^{-1}). The ^{1}H NMR spectrum ($CDCl_3$) of the 1,3-bis(benzyloxy)-*p-tert*-butylcalix[4]arene-crown-5–potassium picrate complex (20% complexation) showed that the cone conformation is present and that most signals are broadened. Attempts to increase the percentage of complexed KPic by adding solid potassium picrate failed. Obviously, the calix[4]arene moiety in the free ligand **4c** is in a cone conformation (vide supra), and **4c** cannot adopt a partial cone conformation due to inhibited ring inversion. The partial cone is the optimal conformation for complexation, and this result demonstrates clearly how small differences in structure may lead to large differences in complex stability.

The increased thermodynamic stabilities of the complexes of **5** with alkali picrates compared to **4b** is a result of the increased rigidity of the 2,6-dianisylpyridine bridge compared to the flexible crown ether bridge. CPK molecular models of **5** show that in the free ligand conformational changes with regard to the *p-tert*-butylcalix[4]arene moiety are possible. Whereas the free ligand is present in a cone conformation (vide supra), the ^{1}H NMR spectra ($CDCl_3$) of the complexes with the most complementary cations (K^+ and Rb^+) show the partial cone conformation. Previously we have shown that pyridohemispherands are flexible, and this was confirmed by X-ray analysis of both the free ligand and the sodium picrate complex.[2,3] Obviously, also in the case of **5**, reorganization prior or upon complexation still is necessary and **5** should be regarded as a hemispherand rather than as a spherand. On the other hand, CPK molecular models do show that the cavity in **5** is shielded from solvent molecules. Extractions of NaPic and KPic from water to a $CDCl_3$ solution of **5** reached equilibrium only in 6–8 h. This observation shows that the rate of association has become slow, and this reflects a high degree of shielding of the cavity of **5** from water molecules.

The isolation of the sodium or potassium bromide complexes of **6** in the synthesis of this novel host molecule already gave a first indication of the high thermodynamic stability of these complexes. The extreme reaction conditions necessary to decomplex **6**·NaBr (vide supra) indicated also a high kinetic stability of the complex. The ^{1}H NMR spectra ($CDCl_3$) of the sodium, potassium, and rubidium picrate complexes (**6**·NaPic, **6**·KPic, and **6**·RbPic) are very similar but minor and significant chemical shift differences were observed. The most remarkable signal in these

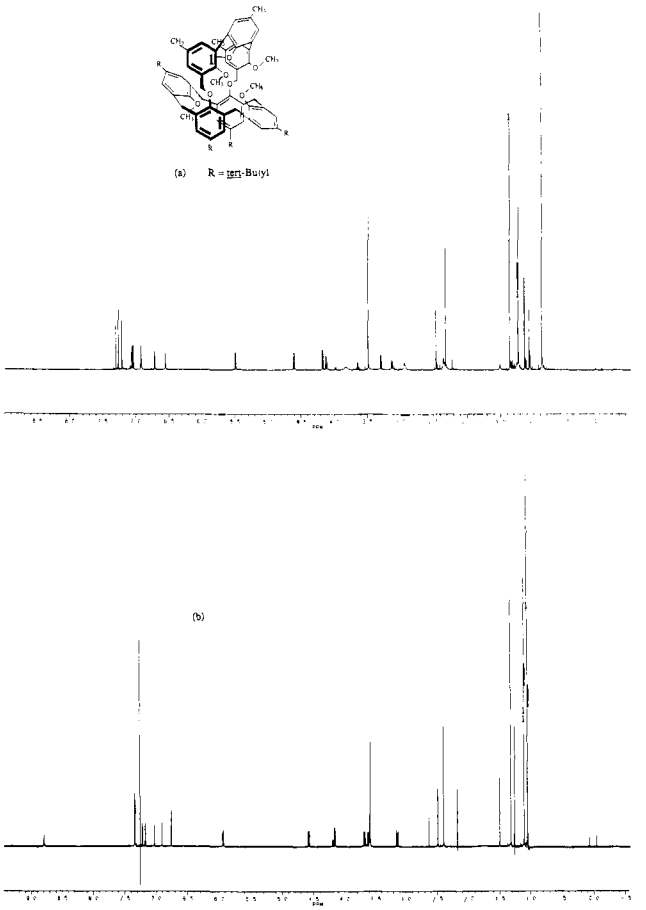

Figure 5. ^{1}H NMR spectra ($CDCl_3$) of **6** (a) and **6**·NaPic (b).

spectra is a singlet at δ –0.05 in **6**·NaPic, at δ 0.04 in **6**·KPic, and at δ 0.20 in **6**·RbPic. This signal (3 H) is attributed to an "endo-positioned" methoxy group of the *p-tert*-butylcalix[4]arene moiety, while in the uncomplexed **6** (partial cone) methoxy absorptions are found at δ 2.95 (vide infra). The downfield shift in the series sodium, potassium, and rubidium complexes is a result of the increasing radius of the cation, which forces the methoxy group more out of the shielding zone of the calix partial cone, which is the favorable conformation for complexation. The other methoxy groups in **6**·NaPic give signals at δ 4.15 (exo-positioned calix[4]arene OCH_3), at δ 3.54 (outer *m*-teranisyl OCH_3), and at δ 1.45 (inner *m*-teranisyl OCH_3). The signals for all the benzylic protons are AB systems. The $ArCH_2O$ hydrogen atoms give an AB pattern at δ 5.89 and 4.11 (J = 11.1 Hz), whereas the calix[4]arene methylene protons are present as doublets as a result of the partial cone conformation (Figure 5).

The calixspherand **6** (free ligand) is present in a flattened partial cone conformation as indicated by the 1:1:2 ratio of the signals from the *tert*-butyl hydrogen atoms. The endo-positioned methoxy group is found at δ 2.95, whereas the exo-positioned methoxy group absorbs at δ 3.82. The outer methoxy groups of the *m*-teranisyl moiety give a signal at δ 3.48, and the inner methoxy group gives an absorption at δ 1.06. From the chemical shift differences, we see that the inverted calix[4]arene aromatic ring with the endo-positioned methoxy group rotates to minimize the steric strain in the free ligand **6**.

In order to determine the thermodynamic stabilities, we performed extraction experiments with **6** and alkali picrates in the two-phase $CDCl_3$–H_2O system. These experiments already indicated a further increase in the shielding of the cavity from solvent molecules compared to the hemispherand **5**.

Complexation of sodium picrate from water to a chloroform solution of **6** gave no equilibrium even after 88 h. Although the less highly solvated potassium ion[15] was complexed faster, no equilibrium was reached in a few days. Complexation of the more

Table V. Complexation (k_c) and Decomplexation (k_d) Rate Constants, Association Constants (K_a), and Binding Free Energies ($-\Delta G°$) for Spherand **6**[a]

guest	temp, K	k_c, $M^{-1}\cdot s^{-1}$	k_d, s^{-1}	$(k_c/k_d)K_a$, M^{-1}	$-\Delta G°$, $kcal\cdot mol^{-1}$
Na^+	358		4.0×10^{-5}		
	343		3.4×10^{-6}		
	328		6.4×10^{-7}		
	298	1.3×10^4	6.0×10^{-9}	2.1×10^{12}	16.8
K^+	358		5.5×10^{-6}		
	353		2.5×10^{-6}		
	348		9.2×10^{-7}		
	298	2.2×10^5	1.0×10^{-8}	2.2×10^{13}	18.1
Rb^+	298	2.5×10^5	6.9×10^{-5}	3.6×10^9	13.0[b]

[a] The extrapolated $\Delta H^{\ddagger}_{298}$ and $\Delta S^{\ddagger}_{298}$ values for Na^+ were 31.0 $kcal\cdot mol^{-1}$ and 8.0 $cal\cdot mol^{-1}\cdot K^{-1}$, respectively, and for K^+, these were 35.0 $kcal\cdot mol^{-1}$ and 22.2 $cal\cdot mol^{-1}\cdot K^{-1}$, respectively. [b] From the two-phase extraction experiment, a $\Delta G°$ value of -12.0 $kcal\cdot mol^{-1}$ was obtained.

weakly solvated rubidium ion gave equilibrium after 24 h, and a K_a value of 8.0×10^8 ($\Delta G° = -12.0$ $kcal\cdot mol^{-1}$) was found. When **6** and lithium or cesium picrate were equilibrated as described above, no changes in the ^1H NMR spectra were observed.

Kinetics of Complexation and Decomplexation of 6–Alkali Picrate Complexes. The rates of complexation of the calixspherand **6** and alkali picrates were determined in a *homogeneous* chloroform solution which was saturated with D_2O. Because these alkali picrate salts are not sufficiently soluble in chloroform, we have used a competition method that we have developed for the study of the kinetics of the complexation of *tert*-butylammonium salts and simple crown ethers[16] and that was also used by Cram et al.[13] for their studies on spherands. The method comprises the exchange of the alkali picrate between a relatively weak complex ($L\cdot M^+X^-$) and a second ligand (**6**) that forms a more stable complex ($K_L \ll K_6$)

$$L + M^+X^- \overset{K_L}{\rightleftharpoons} LM^+\cdot X^-$$

$$\mathbf{6} + M^+X^- \overset{K_6}{\rightleftharpoons} \mathbf{6}\cdot M^+X^-$$

In this case, the free salt concentration is determined exclusively by K_L ($[M^+X^-] = [LM^+\cdot X^-]/K_L[L]$). If the exchange of M^+X^- is slow, the rate-determining step is the complexation of M^+X^- by **6** since the rates of complexation and decomplexation of L with M^+X^- are fast on the appropriate time scale. Because the value of K_a of the complexes of **6** with alkali picrates is at least 10^9 M^{-1}, k_d $[\mathbf{6}\cdot M^+X^-] \ll k_c$ $[\mathbf{6}][M^+X^-]$ and the increase of $[\mathbf{6}\cdot M^+X^-]$ is given by eq 1. In the ^1H NMR spectrum, the relative concen-

$$\frac{d[\mathbf{6}\cdot M^+X^-]}{dt} = k_c\frac{[\mathbf{6}][L\cdot M^+X^-]}{K_L[L]} \quad (1)$$

trations of **6** and the corresponding alkali picrate complexes can be monitored via the absorptions of the endo OCH_3 group, which has a different value for **6** (δ 2.95), **6**·NaPic (δ −0.05), **6**·KPic (δ 0.04), and **6**·RbPic (δ 0.20). The time scale of the exchange process can be selected by the appropriate choice of L. The results of the experiments are summarized in Table V.

The rates of complexation are not very different for Na^+, K^+, and Rb^+, but the absolute values 10^4–10^5 $M^{-1}\cdot s^{-1}$ are much smaller than the rates of complexation of simple crown ethers and salts in chloroform.[16b,17] Cram and Lein reported rates of complexation at 25 °C in chloroform, saturated with 4.1×10^5 $M^{-1}\cdot s^{-1}$ (**1**·NaPic) and 7.5×10^4 $M^{-1}\cdot s^{-1}$ (**1**·LiPic) D_2O.

The rates of *decomplexation* are the most important parameters for our ultimate objective, the design of ligands that form kinetically stable complexes with Rb^+. These rates were experimentally determined by the method that was developed by Cram and Lein[1b] for the spherand (**1**) complexes. Since the endo methoxy group provides an excellent probe, we have synthesized the hexadeuteriocalixspherand (**6**-d_6) by reaction of the 1,3-bis(methyl-d_3)-*p*-*tert*-butylcalix[4]arene (**7b**) and the terphenyl **10**. Assuming that the rate of decomplexation is the rate-determining step in the exchange reaction ($K_a \geq 10^9$ M^{-1}), the rate of decomplexation of the **6**·RbPic complex was determined at 298 K, $k_d = 6.9$ (± 1.3) 10^{-5} s^{-1}.

Table VI. Experimental Data for the X-ray Diffraction Studies

compd	rubidium picrate, **4e**
cryst habit and color	yellow prism
formula	$C_{62}H_{80}N_3O_{15}Rb$
crystal system	triclinic
space group	$P\bar{1}$
cell parameters at 295 K[a]	
a	10.656 (2) Å
b	15.999 (2) Å
c	19.399 (4) Å
α	102.66 (2)°
β	84.14 (3)°
γ	77.48 (2)°
V	3111 (1) Å^3
Z	2
D_{calcd}	1.273 g·cm^{-3}
mol wt	1192.8
cryst dimens	0.2 × 0.3 × 0.1 mm
linear abs coeff	8.36 cm^{-1}
diffractometer	Siemens A.E.D.
diffraction geometry	equatorial
scan type	$\omega - 2\theta$
2θ range	5°–42°
reflections measd	$\pm h,\pm k,l$
total data measd	6958
obsd data measd	4182
unique obsd data	4043
agreement between equiv obsd reflens	0.015
no. of variables	757
overdetermination ratio	5.3
max Δ/σ on last cycle	0.5
R factor	0.106
R_w factor	0.094

[a] Unit cell parameters were obtained by least-squares analysis of the setting angles of 25–30 carefully centered reflections chosen from different regions of reciprocal space.

The rates of decomplexation of the **6**·NaPic and **6**·KPic complexes could not be measured at 298 K because the exchange processes are too slow. From experiments at three different temperatures, we obtained the values for $\Delta H^{\ddagger}$ and $T\Delta S^{\ddagger}$ and extrapolated them to rates of decomplexation at 298 K. The value for **6**·NaPic at 343 K ($k_d = 3.4 \times 10^{-6}$ s^{-1}) can be compared directly with the rate of decomplexation of the corresponding spherand **1**·NaPic complex that was measured by Cram and Lein[13] at the same temperature (1.0×10^{-6} s^{-1}). For KPic and RbPic, no data are available for comparison since these are not complexed by the spherands.

The independently measured values of k_c and k_d allow us to calculate the association constants from experiments in homogeneous chloroform solutions and to compare the value of the **6**·RbPic complex with the K_a as determined by extraction experiments (vide supra). The ratio k_c/k_d of 3.6×10^9 M^{-1} corresponds reasonably well with a K_a value of 8.0×10^8 M^{-1} from the extraction experiments, taking into account the experimental errors in k_c and k_d and the fact that the extraction method does not give a K_a value but an extraction constant $K_e = K_a/K_p$.[18]

The calculated association constants at 298 K for **6**·NaPic and **6**·KPic are 2.1×10^{12} and 2.2×10^{13} M^{-1}, respectively. This means that the free energy of complexation of the *complexation of KPic by the calixspherand* **6** ($\Delta G°_{298} = -18.1$ $kcal\cdot mol^{-1}$) is almost the same as that of the *spherand–NaPic* complex ($\Delta G°_{298} = -19.2$ $kcal\cdot mol^{-1}$).[13]

(16) (a) de Jong, F.; Reinhoudt, D. N.; Smit, C. J.; Huis, R. *Tetrahedron Lett.* **1976**, 4783–4786. (b) de Jong, F.; Reinhoudt, D. N.; Huis, R. *Tetrahedron Lett.* **1977**, 3985–3988.

(17) de Jong, F.; Reinhoudt, D. N. *Stability and reactivity of crown ether complexes*; Academic: London, 1981; pp 31, 95.

(18) Timko, J. M.; Moore, S. S.; Walba, D. M.; Hiberty, P. C.; Cram, D. J. *J. Am. Chem. Soc.* **1977**, *99*, 4207–4219.

(19) Kollman, P. A.; Wipff, G.; Singh, U. C. *J. Am. Chem. Soc.* **1985**, *107*, 2212–2219.

Because the rates of (de)complexation of the 6·MPic complexes are approximately the same in dry chloroform and chloroform saturated with D_2O, it is most likely that the rate-determining step in the complexation reaction is the intrinsic barrier of the unsolvated metal cation penetrating the cavity.[19]

Conclusions. The minor conformational changes observed in the solution of the free ligand **6** upon complexation the sodium, potassium, and rubidium picrates show that the spherand principle can be extended to hosts with larger cavities. The rates of complexation follow the principles of preorganization and desolvation of ligating sites prior to complexation.

Experimental Section

Melting points were determined with a Reichert melting point apparatus and are uncorrected. ^1H NMR spectra were recorded with a Bruker WP-80 spectrometer, and ^{13}C NMR spectra were recorded with a Nicolet MT 200 spectrometer in $CDCl_3$ unless otherwise indicated (Me_4Si as an internal standard). The ^1H NMR spectra of **6** and the corresponding sodium, potassium, and rubidium picrate complexes were recorded on a Bruker AM 600-MHz spectrometer in $CDCl_3$. Mass spectra were obtained with a Varian MAT 311A spectrometer and IR spectra with a Perkin-Elmer 257 spectrophotometer. Absorbance readings in the UV for association constants were taken on a Zeiss M4QIII spectrophotometer. Elemental analyses were carried out by A.M. Christenhusz of the Laboratory of Chemical Analysis of the University of Twente.

Tetrahydrofuran (THF) was freshly distilled from sodium benzophenone ketyl. All reactions in which dry solvents were used were carried out in a nitrogen atmosphere. The chromatographic separations mentioned were performed on silica gel 60 (SiO_2) (E. Merck, particle size 0.040–0.063 mm, 230–240 mesh) or aluminum oxide (Al_2O_3) (E. Merck, neutral grade, particle size 0.063–0.300 mm, 70–230 mesh ASTM).

Fast atom bombardment (FAB) mass spectrometry was carried out using a V. G. MICROMASS ZAB-2HF mass spectrometer, an instrument with reverse geometry, fitted with a high-field magnet and coupled to a V.G. 11/250 data system. The samples were loaded in thioglycerol solution onto a stainless steel probe and bombarded with xenon atoms having 8-keV energy.

26,28-Dimethoxy-5,11,17,23-tetrakis(1,1-dimethylethyl)pentacyclo[19.3.1.1^{3,7}.1^{9,13}.1^{15,19}]octacosa-1(25),3,5,7(28),9,11,13(27),15,17,19(26),21,23-dodecene-25,27-diol (7a). A suspension of **3**–toluene (10.0 g, 13.5 mmol), K_2CO_3 (37.3 g, 270 mmol), and methyl *p*-toluenesulfonate (5.0 g, 27 mmol) in 100 mL of dry acetone (K_2CO_3) was heated under reflux for 24 h. After cooling, the reaction mixture was filtered and the solvent evaporated under reduced pressure to give a white solid. The solid was partitioned between 100 mL of dichloromethane and 100 mL of 0.5 N HCl. The organic phase was washed with water, and the solvent was evaporated under reduced pressure. The residue was submitted to chromatography (SiO_2, CH_2Cl_2–ligroin (40–60) = 4:1 v/v) to give **7a**. The product was identical with previously described **7a**.[11]

5,11,17,23-Tetrakis(1,1-dimethylethyl)-26,28-bis(phenylenemethoxy)pentacyclo[19.3.1.1^{3,7}.1^{9,13}.1^{15,19}]octacosa-1(25),3,5,7(28),9,11,13(27),15,17,19(26),21,23-dodecene-25,27-diol (8). A suspension of **3**–toluene (1.48 g, 2.00 mmol), benzyl *p*-toluenesulfonate (1.05 g, 4.00 mmol), and K_2CO_3 (6.9 g, 0.05 mol) in 100 mL of dry acetone was refluxed for 3 h. After the suspension was cooled to room temperature and filtered, the filtrate was evaporated under reduced pressure. The residue was purified by crystallization from CH_2Cl_2/MeOH: yield 95%, mp 216–220 °C; mass spectrum, *m/e* 828.512 (M^+; calcd 828.512); ^1H NMR δ 7.35–6.90 (m, 10 H, ArH), 7.19 (s, 2 H, OH), 7.03 (s, 4 H, ArH), 6.77 (s, 4 H, ArH), 5.05 (s, 4 H, $ArCH_2O$), 4.28 (d, J = 13.1 Hz, 4 H, $ArCH_2Ar$), 3.41 (d, J = 13.1 Hz, 4 H, $ArCH_2Ar$), 1.29 (s, 18 H, $C(CH_3)_3$), 0.94 (s, 18 H, $C(CH_3)_3$).

Anal. Calcd for $C_{58}H_{68}O_4$: C, 84.02; H, 8.27. Found: C, 83.71; H, 8.41.

29,32-Dimethoxy-2,20,25,35-tetrakis(1,1-dimethylethyl)-6,7,9,10,12,13,15,16-octahydro-28*H*,4,18-(methano[1,3]benzenomethano)-23,27-metheno-22*H*-dibenzo[*n*,*w*][1,4,7,10,13]pentaoxacyclotetracosin (4b). A mixture of **7a** (1.15 g, 1.5 mmol), and sodium hydride (0.15 g, 5 mmol) in 300 mL of dry THF was heated under reflux for 0.5 h. Subsequently a solution of tetraethylene glycol di-*p*-toluenesulfonate (0.76 g, 1.5 mmol) in 50 mL of dry THF was added over a 2-h period. The reaction mixture was heated under reflux for 8 h, and after it cooled, 10 mL of water was added. The solvent was evaporated under reduced pressure, and the residue was partitioned between 50 mL of chloroform and 50 mL of 0.5 N HCl. The organic phase was washed with water, dried ($MgSO_4$), and filtered, and the solvent was evaporated under reduced pressure. The residue was submitted to chromatography (Al_2O_3, chloroform–hexane = 1:9 v/v) to give **4b**. Recrystallization from methanol/chloroform by slow evaporation of the solvent afforded **4b** as colorless crystals: yield 30%, mp 296–298 °C; mass spectrum, *m/e* 834.545 (M^+; calcd, 834.543); ^1H NMR δ 7.13 (s, 4 H, ArH), 6.50 (s, 4 H, ArH), 4.37 (d, J = 12.3 Hz, 4 H, $ArCH_2Ar$), 4.09 (s, 6 H, OCH_3), 4.00–3.50 (m, 16 H, OCH_2CH_2O), 3.14 (d, J = 12.3 Hz, 4 H, $ArCH_2Ar$), 1.34 (s, 18 H, $C(CH_3)_3$), 0.81 (s, 18 H, $C(CH_3)_3$).

Anal. Calcd for $C_{54}H_{68}O_7$: C, 77.66; H, 8.93. Found: C, 78.07; H, 9.03.

2,20,25,35-Tetrakis(1,1-dimethylethyl)-6,7,9,10,12,13,15,16-octahydro-28*H*-(methano[1,3]benzenomethano)-23,27-metheno-29,32-bis(phenylmethoxy)-22*H*-dibenzo[*n*,*w*][1,4,5,10,13]pentaoxacyclotetracosin (4c) was prepared from **8** and tetraethylene glycol di-*p*-toluenesulfonate as described for **4b** to give pure **4c** as white crystals: yield 25%; mp 283–284 °C; mass spectrum, *m/e* 984 (M^+); ^1H NMR δ 7.38 (m, 10 H, C_6H_5), 7.08 (s, 4 H, Ar H), 6.42 (s, 4 H, Ar H), 4.72 (s, 4 H, $ArCH_2$), 4.32 (d, J = 12.9 Hz, 4 H, $ArCH_2Ar$), 4.02 and 3.49 (s, 16 H, OCH_2CH_2O), 3.02 (d, J = 12.9 Hz, 4 H, $ArCH_2Ar$), 1.33 (s, 18 H, $C(CH_3)_3$), 0.81 (s, 18 H, $C(CH_3)_3$).

Anal. Calcd for $C_{66}H_{82}O_7{\cdot}CHCl_3$: C, 72.7; H, 7.56. Found: C, 73.6; H, 7.52.

32,35-Dimethoxy-2,23,28,38-tetrakis(1,1-dimethylethyl)-6,7,9,10,12,13,15,16,18,19-decahydro-31*H*-(methano[1,3]benzenomethano)-26,30-metheno-25*H*-dibenzo[*q*,*z*][1,4,7,10,13,16]hexaoxacycloheptacosin (4e) was prepared from **7a** and pentaethylene glycol di-*p*-toluenesulfonate as described for **4b**. The crude product was purified by preparative TLC (Al_2O_3, ethyl acetate–hexane = 9:1 v/v) to give pure **4e**: yield 50%; mp 253–257 °C; ^1H NMR δ 7.12 (s, 4 H, Ar H), 6.45 (br s, 4 H, Ar H), 4.40 (d, 4 H, Ar CH_2), 4.1–4.3 (m, 26 H, OCH_2 and OCH_3), 3.13 (d, 4 H, Ar CH_2), 1.35 (s, 18 H, $C(CH_3)_3$), 0.80 (s, 18 H, $C(CH_3)_3$).

Anal. Calcd for $C_{56}H_{78}O_8$: C, 76.48; H, 8.95. Found: C, 76.92; H, 8.85.

Rubidium picrate (4e) was prepared by slow evaporation of the solvent of a 1:1 mixture of **4e** in $CHCl_3$ and rubidium picrate in methanol.

9,19-Dimethyl-2,26,31,41-tetrakis(1,1-dimethylethyl)-35,38,44,46-tetramethoxy-22*H*,34*H*,4,24-(methano[1,3]benzomethano)-7,11:17,21:29,33-trimetheno-12,16-nitrilo-6*H*,28*H*-dibenzo[*b*,*k*][1,13]-dioxacyclotriacontin (5). A solution of **9** (0.68 g, 1.35 mmol) and **7a** (0.91 g, 1.35 mmol) in 50 mL of dry THF was added over a 16-h period to a boiling suspension of sodium hydride (0.13 g, 5.4 mmol) in 100 mL of dry THF. After addition, the reaction mixture was refluxed for another 8 h and cooled to room temperature, and 5 mL of water was carefully added. The solvent was removed under reduced pressure, and the residue was partitioned between 25 mL of dichloromethane and 25 mL of 1.0 N HCl. The organic phase was washed with water, dried with $MgSO_4$, and filtered, and the solvent was removed under reduced pressure. The residue was submitted to column chromatography (Al_2O_3, CH_2Cl_2–MeOH = 95:5 v/v) to give pure **5**: yield 20%; mp > 300 °C; mass spectrum, *m/e* 1018.5 (M^+); ^1H NMR δ 7.89–7.44 (m, 3 H, pyridine H), 7.12 (m, 8 H, ArH), 6.50 (s, 4 H, ArH), 5.44 (d, J = 8.6 Hz, 2 H, $ArCH_2O$), 4.65 (d, J = 12.4 Hz, 2 H, $ArCH_2O$), 4.27–4.06 (m, 4 H, $ArCH_2$), 3.27 (s, 12 H, OCH_3), 3.12 (d, J = 12.5 Hz, 4 H, $ArCH_2$), 2.34 (s, 6 H, $ArCH_3$), 1.48 (s, 18 H, $C(CH_3)_3$), 0.82 (s, 18 H, $C(CH_3)_3$).

Anal. Calcd for $C_{69}H_{81}NO_6$: C, 81.22; H, 8.00; N, 1.37. Found: C, 81.42; H, 7.98; N, 1.33.

2,26,31,41-Tetrakis(1,1-dimethylethyl)-35,38,44,45,46-pentamethoxy-9,14,19-trimethyl-22*H*,34*H*,4,24-(methano[1,3]benzenomethano)-7,11:12,16:17,21:29,33-tetramethano-6*H*,28*H*-dibenzo[*b*,*k*][1,13]dioxacyclotriacontin–sodium picrate (6·NaPic) was prepared from **10** and **7a** as described for **5**. The solid, obtained after extraction, was triturated with diisopropyl ether, and 10 mL of methanol was added. The resulting suspension was filtered, and the filtrate was concentrated to give **6**·NaBr as a white solid. The solid was dissolved in 10 mL of chloroform, filtered, and shaken with 10 mL of a 5% sodium picrate solution. The organic phase was separated and the solvent removed under reduced pressure to a small volume, whereupon 3 mL of methanol was added. Slow evaporation of solvent from the clear solution afforded yellow crystals of pure **6**·NaPic: mp > 300 °C; mass spectrum, *m/e* 1063.5 (M^+); ^1H NMR (600 MHz) δ 8.75 (s, 2 H, picrate), 7.30–6.86 (m, 14 H, ArH), 5.92 (d, J = 11.1 Hz, 2 H, $ArCH_2$), 4.53 (d, J = 12.7 Hz, 2 H, $ArCH_2$), 4.11 (d, J = 11.1 Hz, 2 H, $ArCH_2$), 3.63 (d, J = 12.7 Hz, 2 H, $ArCH_2$), 4.15 (s, 3 H, *exo*-OCH_3), 3.54 (s, 6 H, OCH_3), 3.57 (d, J = 15.1 Hz, 2 H, $ArCH_2Ar$), 3.09 (d, J = 15.1 Hz, 2 H, $ArCH_2Ar$), 2.45 (s, 3 H, $ArCH_3$), 2.35 (s, 6 H, $ArCH_3$), 1.27 (s, 9 H, $C(CH_3)_3$), 1.06 (s, 9 H, $C(CH_3)_3$), 1.45 (s, 3 H, OCH_3), 1.00 (s, 18 H, $C(CH_3)_3$), −0.05 (s, 3 H, *endo*-OCH_3).

Anal. Calcd for $C_{78}H_{88}N_3O_{14}$·Na·3H_2O: C, 68.45; H, 6.92; N, 3.07. Found: C, 68.36; H, 6.86; N, 2.68.

6·KPic: ^1H NMR (600 MHz) δ 8.75 (s, 2 H, picrate), 7.35–6.93 (m, 14 H, Ar H), 5.77 (d, J = 11.0 Hz, 2 H, $ArCH_2$), 4.50 (d, J = 12.7 Hz,

2 H, $ArCH_2Ar$), 4.11 (d, J = 11.0 Hz, 2 H, $ArCH_2Ar$), 4.01 (s, 3 H, *exo*-OCH_3), 3.67 (d, J = 15.7 Hz, 2 H, $ArCH_2Ar$), 3.55 (s, 6 H, OCH_3), 3.64 (d, J = 12.7 Hz, 2 H, $ArCH_2Ar$), 3.32 (d, J = 15.7 Hz, 2 H, $ArCH_2Ar$), 2.47 (s, 3 H, $ArCH_3$), 2.36 (s, 6 H, $ArCH_3$), 1.50 (s, 3 H, OCH_3), 1.29 (s, 9 H, $C(CH_3)_3$), 1.04 (s, 9 H, $C(CH_3)_3$), 1.05 (s, 18 H, $C(CH_3)_3$), 0.04 (s, 3 H, *endo*-OCH_3).

6·RbPic: ^1H NMR (600 MHz) δ 8.75 (s, 2 H, picrate), 7.35–6.95 (m, 14 H, Ar H), 5.68 (d, J = 10.8 Hz, 2 H, $ArCH_2O$), 4.48 (d, J = 12.9 Hz, 2 H, $ArCH_2Ar$), 4.09 (d, J = 10.8 Hz, 2 H, $ArCH_2Ar$), 3.92 (s, 3 H, *exo*-OCH_3), 3.72 (d, J = 15.9 Hz, 2 H, $ArCH_2Ar$), 3.62 (d, J = 12.9 Hz, 2 H, $ArCH_2Ar$), 3.55 (s, 6 H, OCH_3), 3.46 (d, J = 15.9 Hz, 2 H, $ArCH_2Ar$), 2.48 (s, 3 H, $ArCH_3$), 2.35 (s, 6 H, $ArCH_3$), 1.72 (s, 3 H, OCH_3), 1.29 (s, 9 H, $C(CH_3)_3$), 1.07 (s, 18 H, $C(CH_3)_3$), 1.06 (s, 9 H, $C(CH_3)_3$), 0.20 (s, 3 H, *endo*-OCH_3).

***p-tert*-Butylcalixspherand (6).** A quartz ampule (20 mL) containing a mixture of **6**·NaBr (0.05 g, 0.043 mmol), 8 mL of water (degassed), and 2 mL of methanol (degassed) was sealed at −70 °C. The ampule was placed up to the meniscus in an oil bath and heated for 3 days at 120 °C. The resulting suspension was cooled to room temperature and filtered, and the white solid was washed with water. Triturating with diisopropyl ether afforded **6**: yield 90%; mass spectrum, m/e 1063.5 (M^+); ^1H NMR (600 MHz) δ 7.24–6.57 (m, 14 H, Ar H), 5.49 (d, J = 9.6 Hz, 2 H, $ArCH_2$), 4.62 (d, J = 12 Hz, 2 H, $ArCH_2$), 4.22–3.05 (m, 8 H, $ArCH_2$), 3.81 (s, 3 H, OCH_3), 3.49 (s, 6 H, OCH_3), 2.93 (s, 3 H, OCH_3), 2.46 (s, 3 H, $ArCH_3$), 2.35 (s, 6 H, $ArCH_3$), 1.36 (s, 9 H, $C(CH_3)_3$), 1.23 (s, 9 H, $C(CH_3)_3$), 1.06 (s, 3 H, OCH_3), 0.87 (s, 18 H, $C(CH_3)_3$).

***p-tert*-Butylcalixspherand-d_6 (6-d_6)** was prepared from **7b** and **10** similarly as described for **6**·NaBr and **6**: yield 16%; mass spectrum, m/e 1068.7 (M^+); ^1H NMR (600 MHz) δ 7.29–6.54 (m, 14 H, ArH), 5.48 (d, J = 9.6 Hz, 2 H, $ArCH_2$), 4.60 (d, J = 12.4 Hz, 2 H, $ArCH_2Ar$), 4.17 (d, J = 9.6 Hz, 2 H, $ArCH_2$), 4.11 (d, J = 13.4 Hz, 2 H, $ArCH_2Ar$), 3.48 (s, 6 H, OCH_3), 3.29 (d, J = 12.4 Hz, 2 H, $ArCH_2Ar$), 3.12 (d, J = 13.4 Hz, 2 H, $ArCH_2Ar$), 2.46 (s, 3 H, $ArCH_3$), 2.31 (s, 6 H, $ArCH_3$), 1.36 (s, 9 H, $C(CH_3)_3$), 1.23 (s, 9 H, $C(CH_3)_3$), 1.06 (s, 3 H, OCH_3), 0.87 (s, 18 H, $C(CH_3)_3$).

Determination of the Rates of Decomplexation of *p-tert*-Butylcalixspherand (6) with MPic in $CDCl_3$.[1b] Solutions of **6**·MPic (0.004 M) and of **6**-d_6 (0.004 M) in $CDCl_3$ (saturated with D_2O at 25 °C) were prepared. Aliquots of each solution (300 μL) were mixed in a NMR tube and equilibrated at the desired temperature. When the temperature at which the measurement was carried out was above 55 °C, the NMR tube was sealed to prevent evaporation of the solvent. The NMR tube was allowed to reach the desired temperature (5–10 min), and ^1H NMR spectra were taken at intervals (10–15 points) over 2–3 half-lives. The time used for the individual points was taken at one-half of the total accumulation time. Equilibration was recorded at 5–10 half-lives. The most accurate method to determine the concentrations of **6** was to expand the peaks of the endo- and or outer-positioned methoxy groups in the ^1H NMR spectra and of one reference peak (the inner methoxy group) to full scale. The ratios of these peaks were determined by weighing the paper after cutting it out.

Determination of the Rates of Complexation of *p-tert*-Butylcalixspherand 6 with MPic in $CDCl_3$. The rates of complexation of **6** with MPic were determined as described by Cram and Lein[1b] for the spherand **1**·MPic complexes. We used as the "donor" ligands for the complexation of NaPic, the hemispherand **12b** ($K_a^{NaPic} = 2 \times 10^9$ M^{-1}); for KPic, the acetylhemispherand **12a**[3] ($K_a^{KPic} = 3.5 \times 10^8$ M^{-1}); and for RbPic, the hemispherand **12b**[7a] ($K_a^{RbPic} = 6.3 \times 10^7$ M^{-1}). The data are given in Table V.

X-ray Diffraction. X-ray measurements were performed on a Siemens A.E.D. single-crystal diffractometer on line with an IBM personal computer using Nb-filtered Mo Kα radiation (λ = 0.7107 Å) and operating in the θ–2θ step scanning mode. The most relevant data collection parameters are displayed in Table VI.

Measured intensities were corrected for Lorentz and polarization effects. No corrections were made for absorption effects. The structure was solved by direct methods using MULTAN 80[20] and refined by blocked full-matrix least-squares method with the SHELX[21] package, using the reflections with $I_{hkl} < 3\sigma(I_{hkl})$ [σ_{hkl} based on counting statistics]. All hydrogen atom positions were calculated with the geometrical constraint C–H = 1.08 Å.

Parameters refined were the overall scaling factor, positional parameters, and anisotropic thermal parameters for all the atoms with the exception of the H atoms and of the two disordered C atoms of the crown for which isotropic thermal parameters were assumed. In the two blocks of full-matrix least squares were refined 469 and 288 parameters, respectively.

The weighting scheme adopted for each reflection was $W = [\sigma(F_o) + gF_o^2]^{-2}$, where g = 0.011 43 was a refined parameter. Scattering factors were taken from *International Tables for X-ray Crystallography*.[22] Geometrical calculations were performed with PARST.[23]

Acknowledgment. We thank J. M. Visser and J. L. M. Vrielink of the Department of Chemical Analysis for recording the ^1H NMR spectra and R. Fokkens (University of Amsterdam) for recording the FAB-MS spectra. These investigations were supported by the Netherlands Technology Foundation (S.T.W., Future Technology Science Branch of the Netherlands Organization for Scientific Research (NWO)) and the EEG Twinning project.

Supplementary Material Available: Tables of coordinates and anisotropic thermal parameters of non-H atoms, coordinates and isotropic thermal parameters of H atoms, bond distances and angles, and selected torsion angles for the crystal structures (8 pages); tables of calculated and observed structure factors (24 pages). Ordering information is given on any current masthead page.

(20) Main, P.; Woolfson, M. M.; Lessinger, G.; Germain, G.; Declerq, G. P. MULTAN 80: *a system of computer programs for automatic solution of crystal structures*; Universities of York and Louvain: England and Belgium, 1980.

(21) Sheldrick, G. M. SHELX: *a program for crystal structure determination*; University of Cambridge: England, 1980.

(22) *International Tables for X-ray Crystallography*; Kynock Press: Birmingham, 1974; Vol. 4.

(23) Nardelli, M. *Comput. Chem.* **1983**, *7*, 95–97.